IEEE Access
Multidisciplinary | Rapid Review | Open Access Journal

Received March 16, 2021, accepted April 1, 2021, date of publication April 5, 2021, date of current version April 14, 2021.

Digital Object Identifier 10.1109/ACCESS.2021.3071273

A Novel Approach for Heart Ventricular and Atrial Abnormalities Detection via an Ensemble Classification Algorithm Based on ECG Morphological Features

HUI YANG[1], (Member, IEEE), AND ZHIQIANG WEI[2]
[1]Department of Computer Foundation, Ocean University of China, Qingdao 266100, China
[2]College of Information Science and Engineering, Ocean University of China, Qingdao 266100, China

Corresponding author: Hui Yang (yanghuiouc@163.com)

This work was supported in part by the Humanities and Social Sciences Project of Chinese Ministry of Education under Grant 17YJC880116, in part by the National Natural Science Foundation of China under Grant 61672475, and in part by the Marine Science and Technology (S&T) Fund of Shandong Province for Pilot National Laboratory for Marine Science and Technology, Qingdao under Grant 2018SDKJ0402.

ABSTRACT In this study, a new approach using a novel ensemble classification algorithm based on ECG morphological features is proposed for accurate detection of heart ventricular and atrial abnormalities. First, the raw ECG signal is preprocessed and the main character waves are detected. Second, a combination of ECG morphological features is proposed and extracted from the selected ECG segments. The proposed feature set contains morphological parameters, morphological visual pattern of QRS complex, and principle components of the third level and fourth level of a four-level Sym8 wavelet-decomposed ECG waveform. Next, a novel ensemble classification algorithm, with the key idea of integrating the knowledge acquired by several popular classification algorithms for this task into an ensemble system, is proposed so that the accuracy and robustness over various arrhythmia types could be improved. Finally, the features are applied to the proposed ensemble classification algorithm for abnormality detection. The proposed approach achieved an overall accuracy of 98.68% when it was validated on fifteen heartbeat types from the MIT-BIH arrhythmia database (MITDB), according to the Association for Advancement of Medical Instrumentation (AAMI) standard. The classification accuracies of the six main types – normal beat (N), right bundled branch blocks beat (R), left bundled branch blocks beat (L), atrial premature beat (A), premature ventricular contractions beat (V), and paced beat (P) are 98.75%, 99.77%, 99.70%, 94.81%, 98.57%, and 99.94%, respectively. The proposed approach proves a solid result in comparison with component classification algorithms as well as recent peer works.

INDEX TERMS Classification, ECG morphology, Feature extraction.

I. INTRODUCTION

According to a recent report of the World Health Organization (WHO), cardiovascular disease (CVD) is the leading cause of noncommunicable disease deaths, which takes an estimated 17.9 million lives each year, accounting for 44% of all deaths from noncommunicable diseases in the world [1]. A great number of cardiac arrests are associated with cardiac arrhythmias, which are caused by abnormal formation and conduction of electrical impulses through the myocardial tissue [2]. Therefore, early and timely detection of cardiac arrhythmia is crucial for saving people's lives.

The heart rhythm is controlled by an electrical impulse originated from the atrial sine node (SA node) located in the right atrium of the heart. The electrical activity propagating all over the heart causes electrical potential difference on the skin surface which could be measured with electrodes added to patient's body surface and graphically recorded in Electrocardiogram (ECG).

ECG is a well-known technique for non-invasively measuring the cardiac activity of a patient. A typical normal ECG cycle is composed of several individual components

The associate editor coordinating the review of this manuscript and approving it for publication was Gang Wang.

(P wave, Q wave, R wave, S wave, T wave, and U wave) and is generally reflected by time-domain features, such as amplitude, duration, interval, and segment [3], as illustrated in Fig. 1. The character waves are formed by the successive atrial depolarization and ventricular depolarization [4]. Since cardiac arrhythmias can alter the origin of the electrical stimulus and the subsequent physiological diffusion in the heart, the heart ventricular and atrial abnormalities could cause irregular waveforms of ECG through which different types of cardiac arrhythmias, e.g., premature ventricular contraction beat (V), atrial premature beat (A), and right bundled branch blocks (R), could be diagnosed.

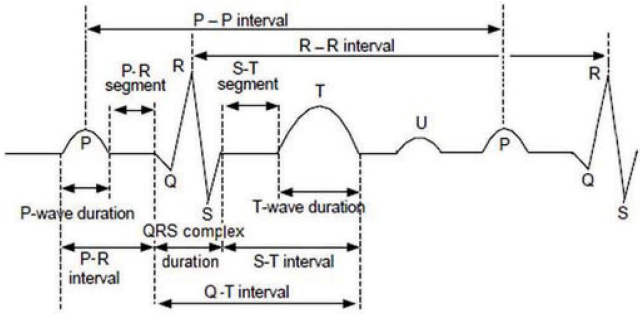

FIGURE 1. A general structure of an ECG signal waveform.

Since it is a tedious process to manually identify heartbeats in long-term ECG recording, computer-aided cardiac arrhythmia detection system provides a high-efficient way for heart ventricular and atrial abnormalities diagnosis.

A. RELATED WORKS

Accurate detection of arrhythmia based on ECG signal depends on the following three steps: 1) preprocessing of the ECG signals, 2) feature extraction, and 3) heartbeat classification.

Since raw ECG signals could be contaminated by interference of various biological and environmental noises, preprocessing should be performed in the first place. A branch of filtering techniques has been successfully applied to the ECG denoising application. The commonly used methods includes wavelet transform [5], [6], band-pass filter [7], empirical mode decomposition (EMD) [8], adaptive filter [9], and independent component analysis (ICA) [10]. For instance, Alqudah *et al*. have applied Butterworth band-pass filters within a range of [0.1, 100] Hz to remove the baseline wander and the high frequency interference [7]. Daubechies wavelet filters have been employed for ECG denoising in [6].

After removing the noises contained in the ECG signals, various features and corresponding extraction methods have been proposed by researchers. In general, features can be extracted from two main sources: original ECG signal (time-domain) and transformations of ECG signal.

The most well-known feature extracted from original ECG signals is the RR interval which is the time interval between two successive R waves [11]. Besides, [12] and [13] have reported that using RR-related features, for example, local-RR and average-RR, can also improve the detection accuracy. The other time-domain features are mainly focused on the morphological variations of the ECG character waves, such as parameters about amplitude, PP interval, PR interval, P-wave duration, QRS-complex duration, slope, area, length of curve, and heart rate variability (HRV) [9], [10], [14]–[21]. For example, an average accuracy of 86.66% in arrhythmia detection was achieved using intervals, amplitudes, and morphological distance by Zhang *et al*. [21]. The main advantage of using amplitudes, intervals and durations as features is that these parametric features have been widely used in clinical practice. However, these measures are very sensitive to noise and do not contain information about the waveform complexity [22].

On the other hand, several features could be extracted through implementing transformation of ECG signal, such as discrete wavelet transform (DWT), power spectrum, hexadecimal local pattern (HLP), and structural co-occurrence matrix (SCM) [16], [23]–[29]. For example, literature [27] has reported that the arrhythmia classification result could be improved via use of power spectrum density of the wavelet-transformed ECG signals. In [25], HLP technique was adopted to extract pattern features from DWT sub-bands of a thousand ECG fragments, resulting an accuracy of 95%. It should be noted that DWT has become as one of the most popular and frequently used methods for ECG feature extraction because of its advantage in multi-resolution analysis [23], [24], [26]. Many statistical features, e.g., mean, variance, and standard deviation, could be calculated from coefficients of DWT [26], [30]. Moreover, ICA, principle component analysis (PCA) and genetic algorithm (GA) were adopted for reducing the dimension of the features [31]–[35]. In [36], an accuracy of 94.52% was obtained in recognition of five heartbeat types using high order spectral (HOS) cumulants with PCA.

Afterwards, the feature vectors are used as input to train an appropriate classifier. Numerous classification algorithms have been adopted for ECG heartbeat classification, for example, support vector machine (SVM) [16], [37], decision tree (DT) [38], [44], logistic regression [39], K-nearest neighbors (KNN) [31], [42], linear discriminant [40], neural network (NN) [16], and neuro-fuzzy system [41], among which KNN, NN, DT, and SVM have been widely used for ECG analysis. Literature [42] reported that a better accuracy (99.30%) was obtained using KNN than NN and SVM in classifying nine types of heartbeats. Jha and Kolekar [43] have employed SVM to classify eight types of heartbeats using the coefficients at the sixth level of tunable Q-wavelet transform as features. Mohanty *et al*. [44] have demonstrated that by using decision tree algorithm based on temporal, spectral, and statistical features, an accuracy of 97.02% was achieved in classification of three types of ventricular arrhythmias. However, due to use of different ECG feature sets, heartbeat types, as well as, different data size, it is not easy to make a direct comparison among these classifiers.

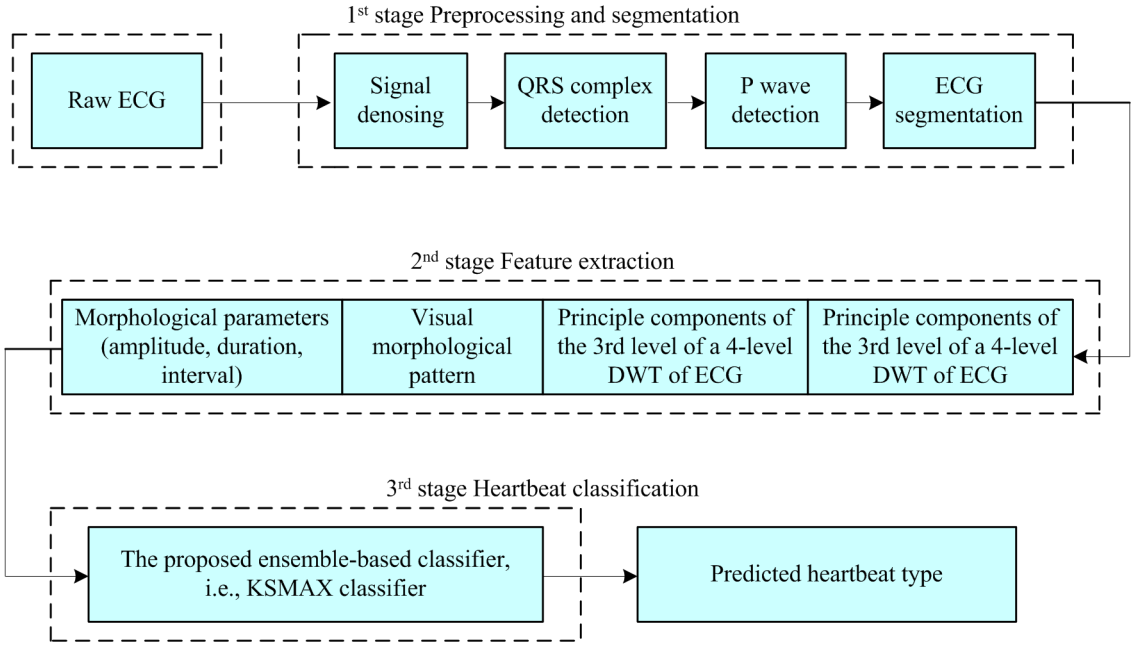

FIGURE 2. The block diagram of the proposed approach.

Recently, many deep-learning based classification approaches, such as convolutional neural network (CNN), have also been applied for ECG heartbeat classification [45]–[49]. For example, Sannino and De Pietro [65] have reported that using a deep neural network (DNN) based classification could obtain promising result on a testing set of two heartbeat types. Literature [47] has achieved 95.78% of accuracy based on CNN in categorizing heartbeats from five types. Deep-learning based approach has the ability to learn abstract features [46]. However, a deep learning approach involves some well-known issues, such as, low interpretability, the necessity of a more extensive database, and requirement of optimization of numerous parameters [16], [49].

Although many studies have shown promising results in cardiac arrhythmia classification, due to differences in theory and the structure of classifiers belonging to different algorithm families, achieving similar results from these classifiers given a common ECG features and training and testing datasets, cannot be expected. In addition, even if the classification accuracy of a classifier for certain type of heartbeat is superior to other classifiers, the performance characteristics may not generalize on other types of heartbeats. On the other hand, many features with mathematical interpretations are lack of physiological meaning and could not allow physicians to comprehend intuitively. Therefore, we still have a long way to go before reliable method could be applied in clinical practice, which implies that more accurate and stable algorithms should be developed.

In order to increase the accuracy and robustness of the classification algorithm, this work proposes a novel approach for detection of heart ventricular and atrial abnormalities using a novel classification algorithm based on ensemble learning and ECG morphological features. And then, the performance of our proposed approach is compared with the component classification algorithms as well as other existing high-performance works.

The main contribution of this paper is summarized as follows: 1) a novel cardiac arrhythmia classification algorithm, called KSMAX, is proposed to increase the classifier's ability of generalizing against various arrhythmia types; 2) extraction of ECG morphological feature sets mostly on physiological meaning to improve interpretability and discriminating capability of the arrhythmia classification system; 3) assessment on a large dataset and 15 heartbeat types; 4) a comparison study of classification performance among several most popular classification algorithms for this task based on the common feature sets and data; 5) a reliable method for cardiac arrhythmia detection with high performance as well as physiological meaning.

II. METHODS

The proposed arrhythmia detection approach is illustrated with a block diagram as shown in Fig. 2. It involves the following three steps: preprocessing and segmentation, ECG morphological feature extraction, and heartbeat classification.

A. PREPROCESSING AND SEGMENTATION

The proposed approach employ the benchmark Pan-Tompkins algorithm [50] in this stage. First, a band-pass filter is used to reduce noise interferences from the raw ECG signals. Next, the slopes of QRS complexes are highlighted using the derivative operator. Then, a squaring operation emphasizes the higher values. Subsequently, a moving window integrator (MWI) acquires the onset, offset, and duration of each QRS complex. At last, the R peak point is attained by applying threshold adjust.

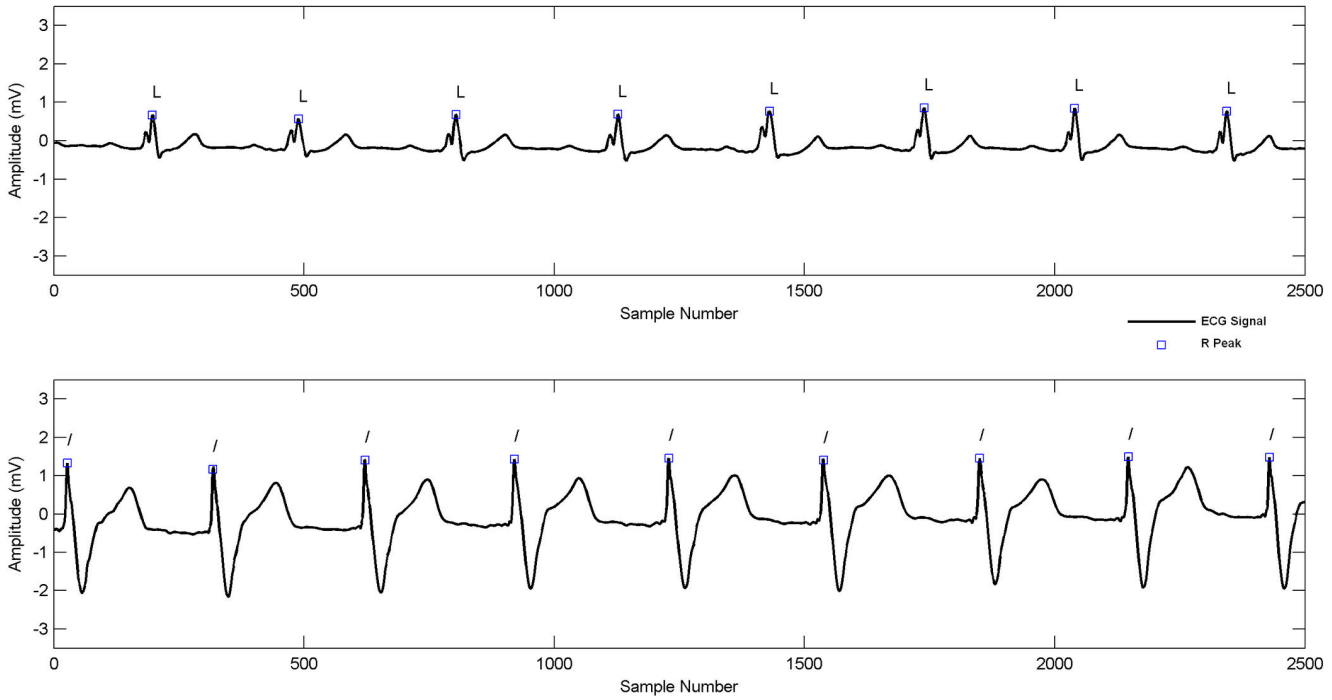

FIGURE 3. Example of ECG pattern for similar arrhythmia with type annotations on each R peak: 'L' and '/' denote left branch block beat and paced beat, respectively.

Since each P wave is of a duration 0.11 ± 0.02 seconds [52], 0.20 seconds (72 samples with a sampling frequency of 360 Hz) before QRS onset are adopted as P wave. The P wave onset and P wave offset are acquired using local distance transform method, while peak point of each P wave is identified as the center of average integral.

B. ECG MORPHOLOGICAL FEATURE EXTRACTION

Unlike normal heartbeat, heartbeat with heart ventricular and atrial abnormalities, such as, blocked areas within ventricle, and ectopic centers, can cause irregular ECG waveforms, through which physicians can diagnose different types of cardiac dysfunctions [20]. In other word, ECG morphology plays an import role in accurate diagnosis. Hence, in order to increase the interpretability of the arrhythmia detection system and to yield prediction results closely to those of the medical experts, this study mainly extract those features with physiological meaning from ECG morphology in various forms.

1) PARAMETER-BASED MORPHOLOGICAL FEATURES

As illustrated in Fig. 1, many clinical studied parametric features could be extracted from character waves.

The morphological parameters of P wave are effective predictors of atrial abnormalities, such as right or left atrial hypertrophy. Therefore, P wave amplitude, P wave duration, and PP interval are contained as features in this work. Besides, PR interval, also referred as PQ interval, which depicts how fast the electrical impulse conducts through the AV (atrioventricular) node to the ventricles, is added to the feature vector as well. Normally, a PR interval ranges from 0.12 to 0.20 seconds [52]. A PR interval longer than normal range usually indicates existence of transmission degradation from the starting of atrial contraction to the onset of the ventricular contraction. Similarly, since QRS complex reflects the electrical activity happening in ventricles, several measures of the QRS complex, including RR interval, R wave amplitude, and QRS duration are selected as the parametric features for detecting ventricular abnormalities.

2) VISUAL-PATTERN-BASED MORPHOLOGICAL FEATURES

As the most remarkable component of an ECG cycle, characteristics of QRS complex are the most utilized. A normal QRS complex is composed of a downward deflected Q wave, an upright R wave, and a downward S wave. However, the morphology of QRS complex could be deeply alternated if the ventricular myocytes contract abnormally. For the same reason, the heartbeats of the same arrhythmia type share similarity in waveform morphology, as illustrated in Fig. 3. Consequently, the QRS-complex morphology has been a stipulated predictor for diagnosing arrhythmias in practice based on ECG [12], [19]. Therefore, it is a routine for medical experts to diagnose various arrhythmias through visually examining the ECG morphology. In order to make advantage of this prior knowledge and analyze the QRS-complex morphological changes as a virtual image, the QRS-complex visual morphology pattern (VMP-QRS) is attained as one of the feature elements in this work, using a K-means based adaptive clustering algorithm [51].

The procedure of obtaining VMP-QRS of each heartbeat is summarized below.

Step 1: Considering the sample frequency of ECG records in MITDB [53] is 360 Hz, segment fifty samples around R peak, with twenty samples before R peak and twenty-nine samples after R peak, as the QRS complex. Then standardize the obtained segments into Z-scores.

Step 2: Place the first instance $\boldsymbol{x}_1$ as the first cluster centroid $\boldsymbol{\mu}_1$ and set the created cluster number C to 1.

Step 3: Assign each instance $\boldsymbol{x}_i$, where $i \in \{1, 2, \ldots, L\}$ and L is the length of dataset, to the cluster $\boldsymbol{\delta}_k$ whose centroid $\boldsymbol{\mu}_k$ has the minimum Euclidean distance $d_{\min}$ to $\boldsymbol{x}_i$, provided $d_{\min}$ is not greater than a threshold T_c; and then execute Step 5. Otherwise, execute Step 4.

Step 4: If C is less than an estimated cluster number C_{max} or $\min\{d(\boldsymbol{\delta}_i, \boldsymbol{\delta}_j)\}$ $(i \neq j)$, i.e., the minimum Euclidean distance between two clusters, is no less than $d_{\min}$, create a new cluster with $\boldsymbol{x}_i$ as the centroid; otherwise, merge the two nearest clusters before set $\boldsymbol{x}_i$ as the centroid of a new cluster.

Step 5: Repeat Step 3 until centroids do not change.

By use of this method, it is possible to cluster QRS segmentations into C patterns, with the number of the centroids (i.e., C) changing adaptively based on the clustering process. When the calculation accomplishes, the cluster label $\boldsymbol{\delta}_i$ which each QRS segmentation $\boldsymbol{x}_i$ is assigned to is used as the visual pattern feature.

3) WAVELET TRANSFORM-BASED MORPHOLOGICAL FEATURES

Wavelet transform is a mathematic tool which decomposes signal into frequencies by maintaining a space location. Many literature has claimed wavelet transform as an efficient method to analyze ECG signal because of its excellent time-frequency localization and multi-resolution analysis characteristics [23], [24], [26]. In this paper, wavelet transform was also adopted to extract efficient morphological features from the most significant ECG character wave, i.e., the QRS complex.

Mathematically, continuous wavelet transform (CWT) is stated as (1):

$$WT_x(a,b) = \langle x(t),\ \psi_{a,b}(t) \rangle = \frac{1}{\sqrt{|a|}} \int_{-\infty}^{+\infty} x(t) \psi^* \left(\frac{t-b}{a} \right) dt \quad (1)$$

where $x(t)$ is the original signal function; $\psi(t)$ represents wavelet basis function; a and b represent dilatation and translation factors, respectively. Since CWT is computationally complex and time-consuming, discrete wavelet transform (DWT) is more often used in practice. If we set $a = 2^j$ and $b = k2^j$, we will obtain the wavelet basis function of DWT as shown in (2):

$$\psi_{j,k}(t) = \frac{1}{\sqrt{2^j}} \psi \left(2^{-j} t - k \right) \quad (2)$$

There are two crucial parameters for the promising feature extraction results: the selection of the wavelet basis function and the number of decomposition levels. In this work, Symlet 8 (Sym8) wavelet basis function was chosen as the wavelet basis function, because it is an approximately symmetric compactly supported wavelet with a shape more similar to the ECG morphology than other wavelet basis functions. The wavelet function and scaling function form of Sym8 wavelet basis function are shown in Fig. 4. On the other hand, considering 90% of the ECG energy distributes among 0.5 Hz to 45 Hz, where the energy of QRS complex is mainly concentrated above the average frequency, a four-level decomposition was utilized in the proposed method. The corresponding pass band width at each level is listed in Table 1.

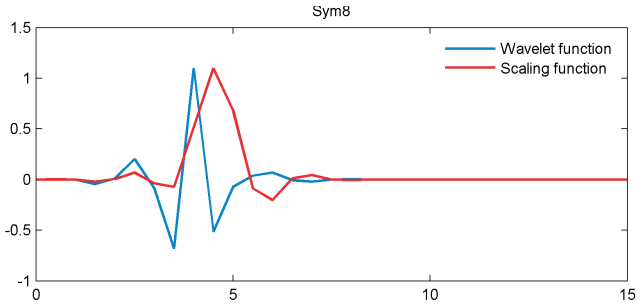

FIGURE 4. Scaling function and wavelet function of the adopted wavelet.

The decomposition of the signal can be implemented by repetitive application of high pass filters and low pass filters. Fig. 5 illustrates a DWT structure based on a two-level decomposition. As can be seen from Fig. 5, original signal a_0 passes through high pass filter g and low pass filter h to produce high frequency sub-band component d_1 and low frequency sub-band component a_1. d_1 and a_1 are named as detail coefficients and approximation coefficients, respectively. The decomposition process in J levels can be represented as (3), (4):

$$a(k,j) = \sum_m a(m, j-1)\, h(m-2k) \quad (3)$$

$$d(k,j) = \sum_m a(m, j-1)\, g(m-2k) \quad (4)$$

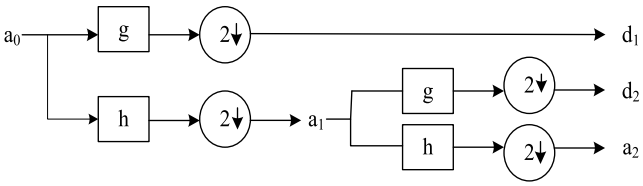

FIGURE 5. DWT structure based on a two-level decomposition.

in which h and g represent scaling function and wavelet function implemented by low pass and high pass filter respectively; and $a(k, j)$ and $d(k, j)$ are the kth approximation and detail coefficients at level j $(j = 1, 2, \ldots, J)$.

Afterwards, the PCA is applied on both the third-level and fourth-level detail coefficients to derive the important information as several orthogonal principal components.

TABLE 1. Pass band widths of the 4-level decomposition of ECG signal.

Level	Low frequency pass band (Hz)	High frequency pass band (Hz)
1	0~90	90~180
2	0~45	45~90
3	0~22.5	22.5~45
4	0~11.25	11.25~22.5

The main steps to perform PCA are as follows:

Step 1: Calculate the covariance matrix $\boldsymbol{C}$ from the data $\boldsymbol{x}$ and its mean vector $\bar{\boldsymbol{x}}$ according to (5):

$$\boldsymbol{C} = (\boldsymbol{x} - \bar{\boldsymbol{x}})\,(\boldsymbol{x} - \bar{\boldsymbol{x}})^{\mathrm{T}} \tag{5}$$

Step 2: Determine the eigenvalues and eigenvectors of matrix $\boldsymbol{C}$. Arrange the eigenvalues λ in descending order, for example, $\lambda_1 \geq \lambda_2 \geq \ldots \geq \lambda_p$. Arrange eigenvectors corresponding to the eigenvalues as $\boldsymbol{l}_1, \boldsymbol{l}_2, \ldots, \boldsymbol{l}_p$, then the jth principal component $\boldsymbol{F}_j$ could be calculated by (6):

$$\boldsymbol{F}_j = \boldsymbol{l}_j^{\mathrm{T}}\boldsymbol{x} \quad (j = 1,\ 2,\ \ldots, p) \tag{6}$$

Step 4: Calculate the contribution rate (i.e., variance explained rate) Cr_j of the jth principal component and the accumulative contribution rate Acr_j (i.e., accumulative variance explained rate) of the first j principal components by (7) and (8), respectively:

$$Cr_j = \frac{\lambda_i}{\sum_{k=1}^{p}\lambda_k} \quad (j = 1,\ 2,\ \ldots, p) \tag{7}$$

$$Acr_j = \frac{\sum_{k=1}^{j}\lambda_k}{\sum_{k=1}^{p}\lambda_k} \quad (j = 1,\ 2,\ \ldots, p) \tag{8}$$

In this work, we chose the principle components with Cr value above 1% as the features of the corresponding sub-bands.

C. HEARTBEAT CLASSIFICATION

The classification stage is vital to the accurate detection of heart ventricular and atrial abnormalities. Although studies have reported promising results obtained using the popular classification algorithms, these classification algorithms may attain different degree of success due to the fact that each classification algorithm solves the recognition problem with different structure and theory. Besides, it should be noted that superior discriminating capability of an appropriately designed classification algorithm to other rival classification algorithms on certain type of heartbeat, cannot be expected on other types of heartbeat arrhythmia.

To improve the entire classification performance, one solution is to integrate the knowledge acquired by the different classification algorithms to increase the robustness against uncertainties of datasets and arrhythmia types. To this end, a novel ensemble classification algorithm which integrates several types of popular classification algorithms for ECG heartbeat classification task is proposed in this work. The principles of each component classification algorithm and our proposed ensemble classification algorithm are described below.

1) NN

The NN is able to approximate certain function $\boldsymbol{Y}$ though adjusting network weights among a set of inter-connected perceptrons. For the implementation of neural network, the multi-layer feed-forward perceptrons (MLP) was adopted in this work. Suppose $\boldsymbol{X}$ is the input data, then the output at iteration k, i.e., $\boldsymbol{Y}_k$, can be defined as (9):

$$\boldsymbol{Y}_k = f(\boldsymbol{X},\ \boldsymbol{W}_k), \tag{9}$$

where $\boldsymbol{W}_k$ represent the network weights upgraded according to (10):

$$\boldsymbol{W}_{k+1} = \boldsymbol{W}_k - \left[\boldsymbol{J}^T\boldsymbol{J} + \mu\boldsymbol{I}\right]^{-1}\boldsymbol{J}^T\boldsymbol{e}, \tag{10}$$

in which $\boldsymbol{J}$ represents the Jacobian matrix with first derivative of errors $\boldsymbol{e}$ in terms of the weight and μ is a dynamic parameter [54]. In this study, a MLP model consisting of one input layer, one hidden layer with 28 perceptrons, and one output layer was adopted by trial and error method. The training stage was terminated after a fixed number of iterations (200).

2) SVM

SVM is well known as an efficient method widely used in classification tasks. The SVM works in the high-dimension feature space with a separating hyperplane. The separating hyperplane is optimized in a way to maximize the distance between the closest representatives of both classes and minimize the empirical classification error [55]. Finally, the optimal separating hyperplane can be represented by a decision function formulated as (11), (12):

$$Y = \sum \boldsymbol{w}_i K\,(\boldsymbol{x}, \boldsymbol{x}_i) + b \tag{11}$$

$$K\,(\boldsymbol{x}, \boldsymbol{x}_i) = \exp\left(-\gamma\,\|\boldsymbol{x} - \boldsymbol{x}_i\|^2\right), \tag{12}$$

where $\boldsymbol{x}_i$ denotes an instance of dataset $\{\boldsymbol{x}_i, i = 1, 2, \ldots, M\}$, $K(\boldsymbol{x}, \boldsymbol{x}_i)$ represents kernel function, $\boldsymbol{w}_i$ is the synaptic weight of the network generated by Lagrange multiplier, b is the bias term [56].

This work uses LIBSVM [57] for building up a SVM classifier. The error penalty factor C that controls overfitting was set as 32 and γ was equal to 0.02.

3) KNN

KNN is a popular supervised classification algorithm based on instance [58]. During the classification process, an instance $\boldsymbol{x}$ is categorized based on the closeness of the K-nearest training instances accessible in the feature space to that instance. There are several distance metric forms used to measure the distance between two instances $\boldsymbol{x}_i$ and $\boldsymbol{x}_j$. In this work, Euclidean distance was used as the distance metric, which is formulated as (13):

$$d\left(\boldsymbol{x}_i, \boldsymbol{x}_j\right) = \left(\sum_{k=1}^{p} \left(\boldsymbol{x}_i\left(k\right) - \boldsymbol{x}_j\left(k\right)\right)^2\right)^{1/2} \tag{13}$$

where p denotes the dimension of the instance. The vector $\boldsymbol{x}$ is classified to the nearest class which has the major votes of the K-nearest neighbors. The appropriate K value was concluded to be 31 at which the best accuracy for the test samples was obtained in evaluation.

4) ADABOOST

Adaptive Boosting (AdaBoost) is a well-known and widely used boosting algorithm, belonging to the category of ensemble learning [59]. The main idea of boosting method is to train a series of weak classifiers iteratively to attain a more accurate prediction than that of a single weak classifier. In AdaBoost algorithm, weak classifiers can be focused on the misclassification instances by assigning higher weights on those incorrectly classified instances from the training set. In this work, DT was adopted as the base classifier of the AdaBoost because DT is a popular classification algorithm used for ECG heartbeat classification as well as a typical selection for AdaBoost. The optimal parameters, learning rate and the maximum number of iterations was found to be 0.1 and 200 using cross validation and grid search.

5) XGBOOST

The eXtreme gradient boosting (XGBoost) is an optimized scalable tree boosting system originally developed by Tianqi Chen as an enhancement to the gradient boosting algorithm [60]. In the machine learning world, XGBoost algorithm has been a well-received tool which solves many data science problems in a fast and accurate way. XGBoost utilizes sequences of DTs that seek to generate a strong classifier. The residual algorithm principle is applied to iteratively generate a new DT using the residual of the prior tree as the target variable for the current tree. In addition, regularization items are added to the loss function to control the complexity of the XGBoost model. Also, XGBoost is capable of parallel processing so that the speed of the algorithm is greatly improved. In this study, the parameters of the XGBoost model, including, learning rate, maximum depth of the decision tree, and maximum number of iterations were concluded to be 0.1, 8, and 150, respectively, with which the best accuracy was achieved in grid search.

6) THE PROPOSED ENSEMBLE CLASSIFICATION ALGORITHM

The main idea of ensemble learning is to attain a better generalization capability, as well as to decrease prediction error of learning algorithms by integrating a set of component classifiers into one ensemble system. Since different types of classifiers perceive a recognition task with their own appropriate inherent structures and theories, this work proposes a novel classification algorithm based on ensemble learning for combining the knowledge acquired by the component classifiers so that the classification performance over various arrhythmia types could be improved.

The selection of component classifiers is vital to the success of the entire ensemble learning algorithm. In this work, we select SVM, KNN, NN, and DT-based AdaBoost, and XGBoost as the component classifiers due to two reasons. First, although the weak algorithm could categorize instances better than random, strong algorithm classify instances more accurately. Hence, in practical applications, strong algorithms are often chosen as the component classifiers. As to the ECG classification scenario, SVM, KNN, NN, and DT are four of the most popular algorithms found in literature for this task. Selecting component classifiers based on these four strong algorithms is favorable to involve less component classifiers and could learn from some existing experience, establishing good prospects for integration their results. Second, these classifiers are heterogeneous with diverse structures and theories, which means the correlation among the predictions of these classifiers is relatively low and could facilitate the improvement of the robustness and generalization capability.

After selection of the component classifiers, a stacking ensemble technique is adopted to combine the prediction of each component classifier. Stacking aims at correcting the errors of the component classifiers by building a meta-classifier with the outputs of the base classifiers as the metadata to predict the final results [61].

The proposed classification model of this paper is composed of two layers of classifiers, as illustrated in Fig. 6. The first level consists of KNN, SVM, MLP, and DT-based Adaboost. The XGBoost algorithm is chosen as the meta-classifier of the second level considering its benefits of efficiency, accuracy, and fast speed. Therefore, we use the combination of initial letter of each component classifier, i.e., KSMAX (KNN-SVM-MLP-AdaBoost-XGBoost), to represent our proposed ensemble classifier in this paper. The feature vectors are used as input of the four base classifiers whose predictions are fed into the second-level classifier, i.e., XGBoost, as input data. The output of the second-level classifier is considered as the final prediction of the KSMAX model.

However, if the base classifiers are trained on the full training data and produce predictions as the input for the meta-classifier training, there will be risk of overfitting. Therefore, the training and testing procedure in this work is optimized using the following method so that the stability and reliability of the entire stacking model could be improved.

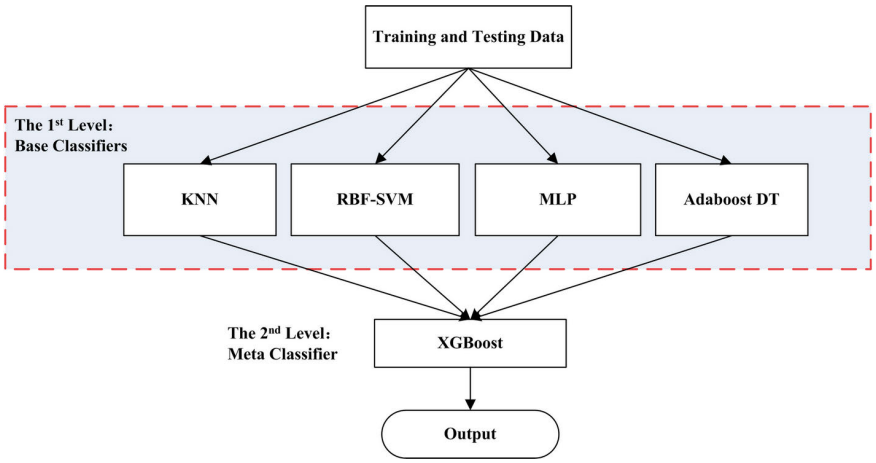

FIGURE 6. The proposed KSMAX ensemble model.

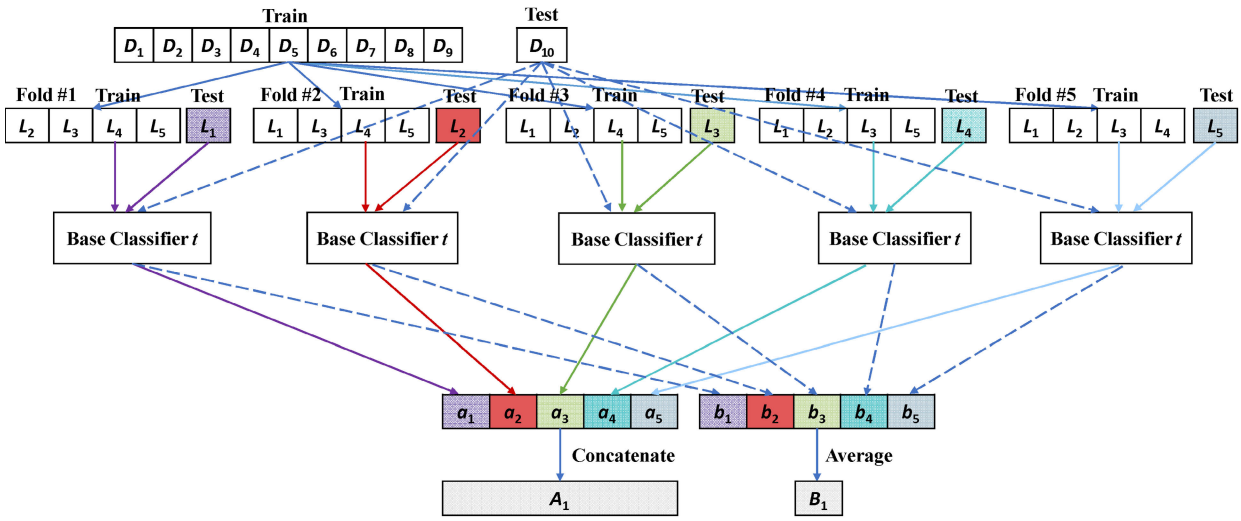

FIGURE 7. The diagram of the training and testing process of a single base classifier (e.g. classifier t) of the proposed KSMAX classification algorithm.

Fig. 7 illustrates the training and testing process of a single base classifier t ($t \in \{1, 2, \ldots, 4\}$) in this work. Assume $\boldsymbol{L} = \boldsymbol{D}_1 \cup \boldsymbol{D}_2 \cup \ldots \cup \boldsymbol{D}_9$ and $\boldsymbol{D}_{10}$ represent the subsets for training and testing respectively in one fold of a ten-fold cross validation method. To train and test the base classifier t, the training data $\boldsymbol{L}$ is randomly partitioned into five subsets, namely, $\boldsymbol{L} = \boldsymbol{L}_1 \cup \boldsymbol{L}_2 \cup \ldots \cup \boldsymbol{L}_5$, $\boldsymbol{L}_i \cup \boldsymbol{L}_j = \emptyset\, (i, j \in \{1, 2, \ldots, 5\}, i \neq j)$ based on a five-fold cross validation method. As shown in Fig. 7, each fold of the five-fold cross validation can be divided into two steps. In the first step, retain a single subset (e.g., $\boldsymbol{L}_j, j \in \{1, 2, \ldots, 5\}$) as the validation data for testing, and train the base classifier t using the remaining four subsets $\boldsymbol{L}_i (i \neq j)$. In the second step, apply two datasets on classifier t for testing: 1) the retained subset $\boldsymbol{L}_j$, generating output $\boldsymbol{a}_j$; and 2) $\boldsymbol{D}_{10}$, generating output $\boldsymbol{b}_j$.

This two-step process is repeated five times, obtaining several outputs, i.e., $\boldsymbol{a}_1, \boldsymbol{a}_2, \boldsymbol{a}_3, \boldsymbol{a}_4$, and $\boldsymbol{a}_5$ as well as $\boldsymbol{b}_1, \boldsymbol{b}_2, \boldsymbol{b}_3, \boldsymbol{b}_4$, and $\boldsymbol{b}_5$. Hence, to concatenate the $\boldsymbol{a}_1, \boldsymbol{a}_2, \boldsymbol{a}_3, \boldsymbol{a}_4$, and $\boldsymbol{a}_5$, we could attain the complete testing results (denoted as $\boldsymbol{A}_1$) on the training dataset $\boldsymbol{L}$, with each of the five subsets used exactly once as the validation data. The five predictions of $\boldsymbol{D}_{10}$, i.e., $\boldsymbol{b}_1, \boldsymbol{b}_2, \boldsymbol{b}_3, \boldsymbol{b}_4$, and $\boldsymbol{b}_5$, can be averaged to produce a single prediction (denoted as $\boldsymbol{B}_1$) of $\boldsymbol{D}_{10}$ from base classifier t.

Above is the complete training and testing process of a single base classifier t ($t \in \{1, 2, \ldots, 4\}$) in this study. Since there are four base classifiers, after performing this process on each base classifier, we could obtain the training dataset for the second-level classifier by concatenating horizontally the generated $\boldsymbol{A}_1, \boldsymbol{A}_2, \boldsymbol{A}_3$, and $\boldsymbol{A}_4$. Similarly, the testing dataset of the second level can be produced by concatenating horizontally the generated $\boldsymbol{B}_1, \boldsymbol{B}_2, \boldsymbol{B}_3$, and $\boldsymbol{B}_4$. Then, the second-level classifier can be trained and tested with these data and yield the final predictions.

III. EXPERIMENTAL RESULT

The arrhythmia heartbeats were classified using the proposed feature set and KSMAX classification algorithm as described in the previous sections.

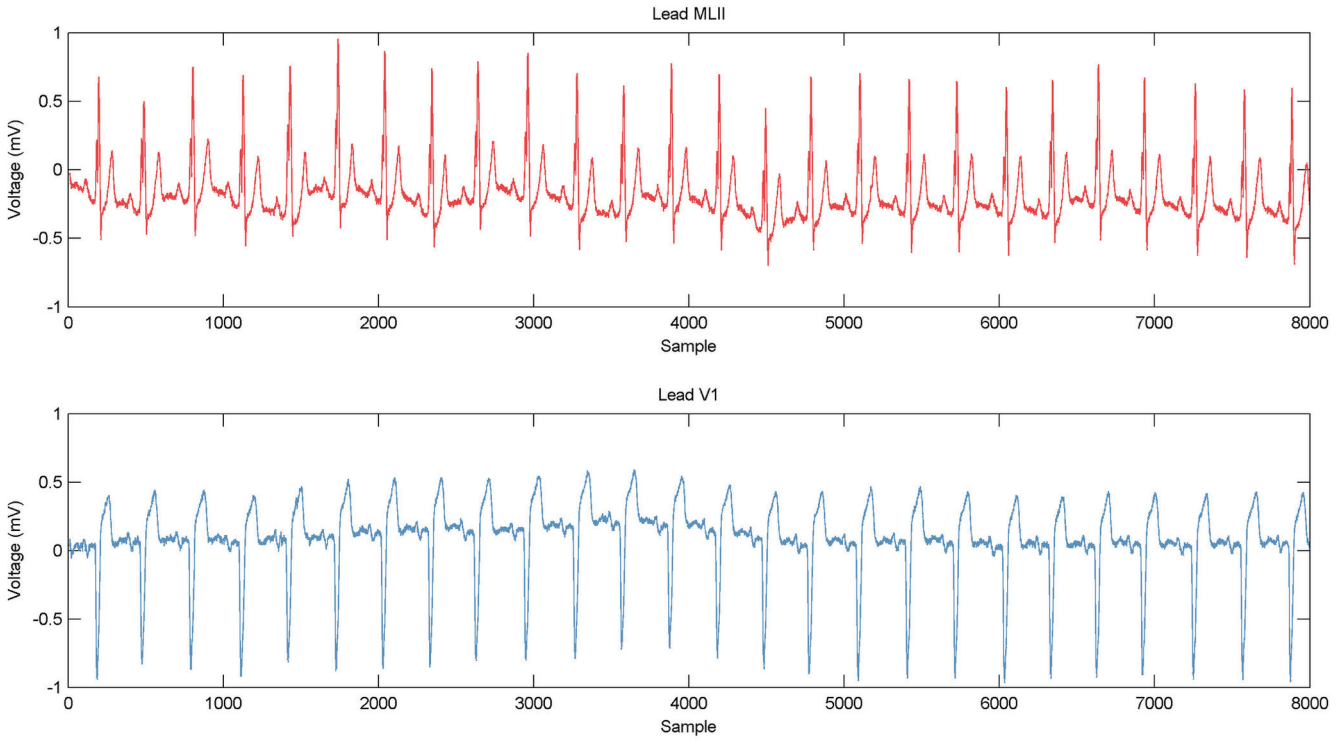

FIGURE 8. The ECG signal example with lead MLII and lead V1 from MITDB.

A. ECG DATA DESCRIPTION

In this study, we adopted realistic ECG data from MITDB [53] to validate the effectiveness of our proposed method for atrial and ventricular abnormalities detection. The MITDB consists of ECG recordings of 47 patients. Each ECG recording contains two channels, lead MLII and V1 (sometimes V5, V2 or V4). One segment of recordings from the MITDB is depicted in Fig. 8. Considering the character waves corresponding to the ventricular and atrial abnormalities are highlighted by lead MLII, the lead MLII is one of the most utilized lead and was also adopted in this study. The heartbeat types from MITDB are mapped to AAMI standard [62]. In this study, all of the 15 heartbeat types compatible with AAMI standard were involved, with a total of 104986 heartbeats obtained with proposed feature set from the MITDB. The distribution of these heartbeats is presented in Table 2.

B. EVALUATION METRICS

The ten-fold cross validation was applied to evaluate the classification performance. During each fold, the training and testing of each level of the KSMAX model was performed in the way as described in Section II. C. 6). When the ten-fold cross validation accomplished, accuracy (Acc), precision (P+), and F_1 score could be calculated by four concepts: true positive (TP), false positive (FP), true negative (TN), and false negative (FN), as defined in (14), (15), and (16):

$$\text{Acc} = \frac{\text{TP} + \text{TN}}{(\text{TP} + \text{FP} + \text{TN} + \text{FN})} \tag{14}$$

$$\text{Precision} = \frac{\text{TP}}{(\text{TP} + \text{FP})} \tag{15}$$

$$\text{F}_1 \text{ score} = \frac{\text{Precision} \times \text{Recall}}{(\text{Precision} \times \text{Recall})} \times 2 \tag{16}$$

in which Recall could be calculated according to (17), representing the ratio of true positives to all instances in actual True class.

$$\text{Recall} = \frac{\text{TP}}{(\text{TP} + \text{FN})} \tag{17}$$

C. RESULTS

In our proposed approach, morphological features, namely, parameters, principle components of detail coefficients, and VMP-QRS, were used as input of the KSMAX model. To better investigate the improvement of discrimination capability in our proposed feature vectors, we grouped features into two feature sets, i.e., the classical ECG parameters (feature set1) and the combination of principle components of detail coefficients and VMP-QRSs (feature set2).

After performing PCA on sub-band detail coefficients of the DWT, there were eleven principle components obtained as features. An example of the detail coefficients attained in the four-level decomposition of a random ECG signal segment is illustrated in Fig. 9. As shown in Fig. 9, the morphological information of QRS complex was concentrated on decomposition level of three and four. Fig. 10 shows the resulting *Cr* and *Acr* of the derived principle components. From the third-level detail coefficients, the first six principle components with the *Cr* value above 1% were regarded as six features in this work. The accumulative variance they explained

TABLE 2. The corresponding relationship between AAMI standard and heartbeat types in the MITDB as well as the summary of the data size adopted in this study.

AAMI Class	MIT-BIH Annotation	Type	Total # of Heartbeats
Normal (N)	N	Normal beat	74722
	L	Left bundle branch block beat	8069
	R	Right bundle branch block beat	7250
	e	Atrial escape beat	16
	j	Nodal escape beat	229
Supraventricular ectopic beat (SVEB)	A	Atrial premature beat	2544
	a	Aberrated atrial premature beat	150
	J	Nodal (junctional) premature beat	83
	S	Supraventricular premature beat	2
Ventricular ectopic beat (VEB)	V	Premature ventricular contraction beat	7122
	E	Ventricular escape beat	106
Fusion beat (F)	F	Fusion of ventricular and normal beat	802
Unknown beat (Q)	P or /	Paced beat	3616
	f	Fusion of paced and normal beat	260
	Q	Unclassifiable beat	15
		Total # of Heartbeats	104986

was up to 97.86%, which means most of the morphology alternation information was retained while the feature dimension has been effectively reduced. Similarly, the first five principle components, with the Cr values above 1% and an Acr value of 98.92%, were attained as morphological features from the fourth-level detail coefficients.

As to the visual morphological pattern feature, the parameter $C_{\max}$ was set to 15 because fifteen heartbeat types were involved in the study and heartbeats from each type have generally similar-looking morphology. However, it should be noted that the number of clusters could change during the clustering process. The choice for T_c was concluded to be 0.78. As a result, there are 21 VMP-QRSs obtained. Some extracted VMP-QRSs are presented in Fig. 11, with gray line representing the centroid of each pattern; while lines in other colors representing original QRS complex segments assigned to the corresponding patterns. Therefore, feature set2 consisted of twelve features, representing eleven principle components and one visual morphological pattern.

The accuracies obtained with our proposed KSMAX classifier and component classifier using different feature sets are given in Table 3, which indicates that the proposed morphological features (feature set1 & set2) produced a better classification result compared to the classical ECG parameters.

To further compare the classification performance of the KSMAX classifier with the component classifiers, the classification accuracies with respect to heartbeat type and feature set are visualized in Fig. 12.

The results of F_1 score and P+ using the proposed approach are summarized in Table 4. To better understand the classification performance, the F_1 score and P+ measures of the MLP, SVM, KNN, AdaBoost, XGBoost and KSMAX with respect to heartbeat type are visualized in Fig. 13 and Fig. 14, respectively.

IV. DISCUSSION

This paper provides a novel approach for heart ventricular and atrial abnormalities detection using a novel ensemble classifier based on ECG morphological features. In general, the experimental results have verified the effectiveness of the proposed method. In the following, we present the discussion of the raised approach in details.

A. PERFORMANCE OF THE PROPOSED APPROACH

As shown in Fig. 12, all classifiers obtained a remarkable improvement in classification accuracy using the proposed feature set (i.e., feature set1 & set2) than that of using classical parameters, with an increasement of 13.32%, 13.26%, 12.04%, 11.47%, 10.22%, and 8.43% for MLP, SVM, KNN,

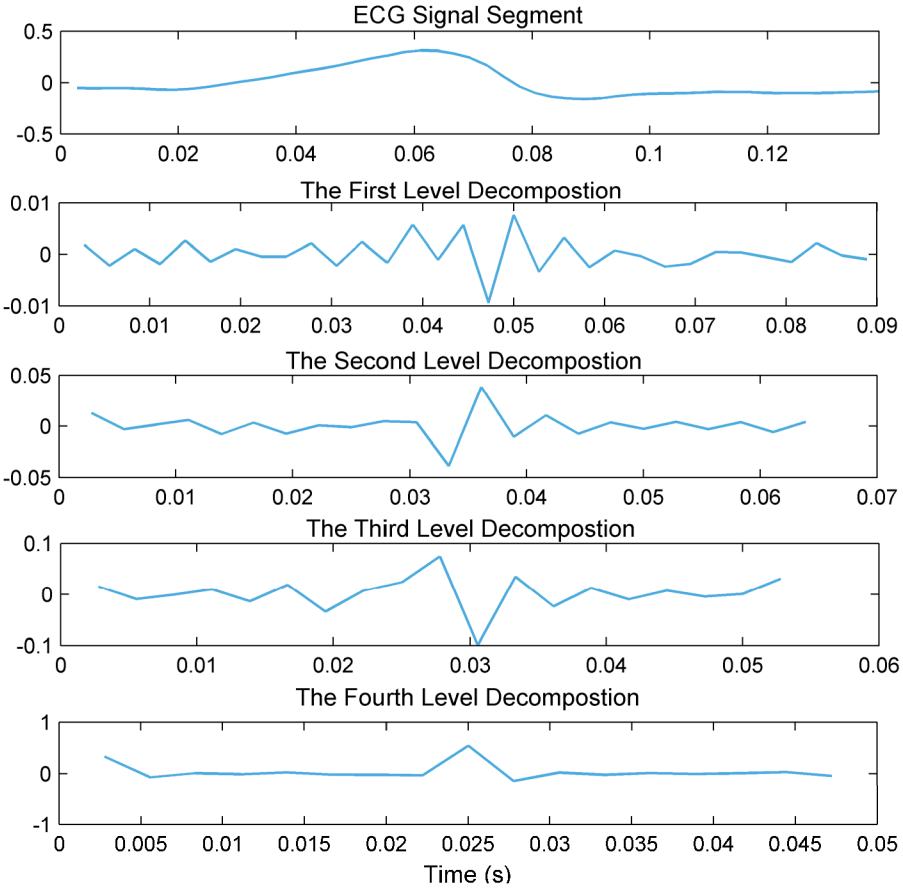

FIGURE 9. Four-level decomposition (detail coefficients) of the ECG signal using Sym8 wavelet basis function.

AdaBoost, XGBoost, and KSMAX, respectively. The best result in terms of the overall accuracy was 98.68% achieved using our proposed KSMAX classifier and feature set. These results indicate that the raised approach is effective in this task for atrial and ventricular abnormalities detection.

One explanation for this result is because the extracted ECG morphological features is efficient in reflecting hidden information in the ECG recordings. The VMP-QRS examples illustrated in Fig. 11 imply that abnormal conduction in ventricle can cause dramatic alternation in ECG morphology. Consequently, the VMP-QRS is efficient in distinguishing one heartbeat type from others in shape. In addition, VMP-QRS can be used as a visual medical predictor for a long-term ECG-based arrhythmia diagnosis.

Moreover, the extracted visual morphological patterns also allow the doctors to comprehend intuitively because doctors routinely infer and diagnose arrhythmia type in way of visually examining ECG morphology patterns. As to the eleven features extracted through PCA and DWT, we visualize some feature examples (principle components) of eight normal (N) and premature ventricular contraction (V) heartbeats from the third and fourth level of detail coefficients in form of heatmap in Fig. 15. As illustrated in Fig. 15(a) and (b), the first principle components of the eight premature ventricular contraction (V) heartbeats are much lighter in color than the counterparts of normal heartbeats. Whereas, the fifth principle components in Fig. 15(b) are much darker than those in Fig. 15(a). Similar contrast in color can also be found in the first and fourth principle components in Fig. 15(c) and (d). Other principle components of the normal and premature ventricular contraction have less but still notably difference in color. These differences further verify their discriminating power in this arrhythmia classification study.

The proposed classifier, i.e., KSMAX, contributed to the classification result as well. Utilizing KSMAX and the proposed feature set, the accuracies for the six main heartbeat types, namely, N, L, R, V, A, and P, that consist of roughly 98.41% of all samples, were 98.75%, 99.70%, 99.77%, 98.57%, 94.81%, and 99.94%, respectively. As demonstrated in Fig. 12, the proposed KSMAX classifier is superior to the component classifiers in overall accuracy. In addition, this advantage does generalize for both feature sets and almost all heartbeat types. Hence, the reliability and effectiveness of the propose KSMAX classifier is verified.

From assessment with respect to the F_1 score, as shown in Fig. 13, using the proposed approach has obtained the highest F_1 score for almost all the types. Especially, compared to

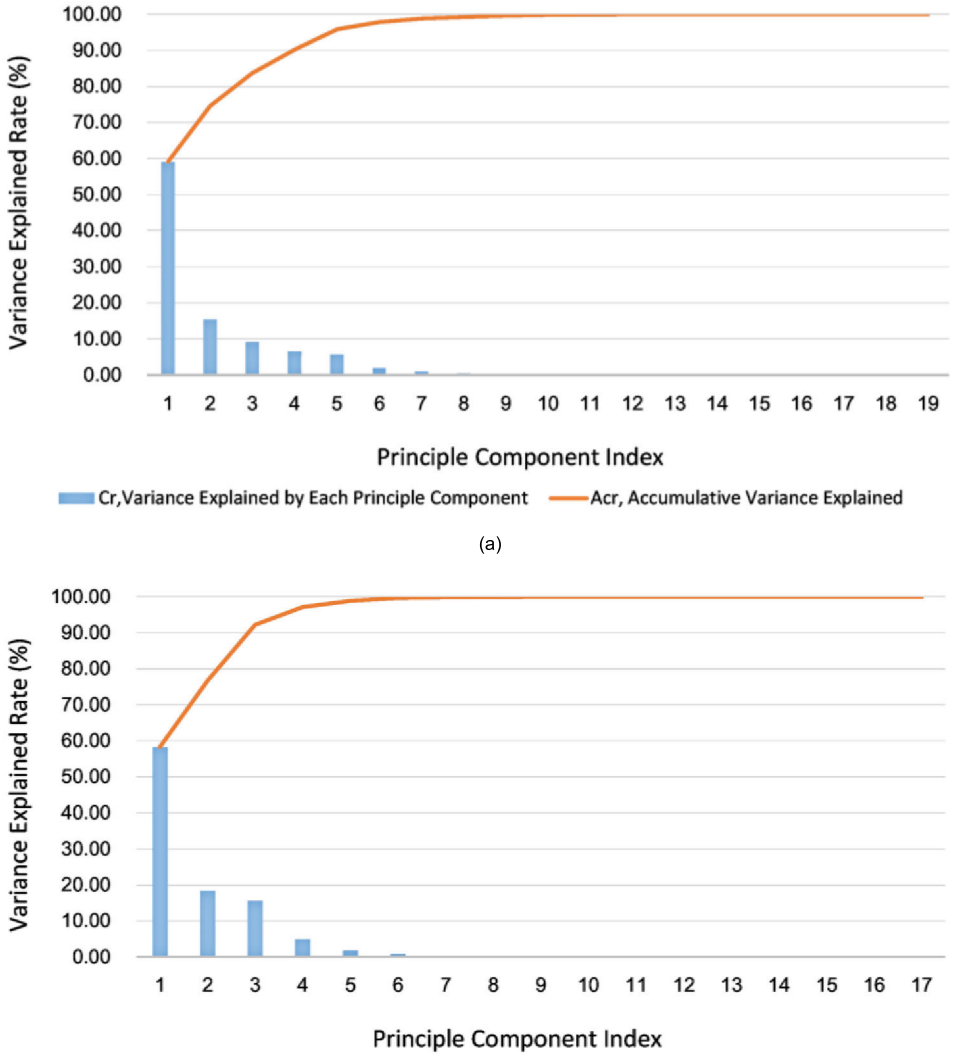

FIGURE 10. Variance explained rates of the principle components from the third-level detail coefficients (a) and the fourth-level detail coefficients (b), respectively.

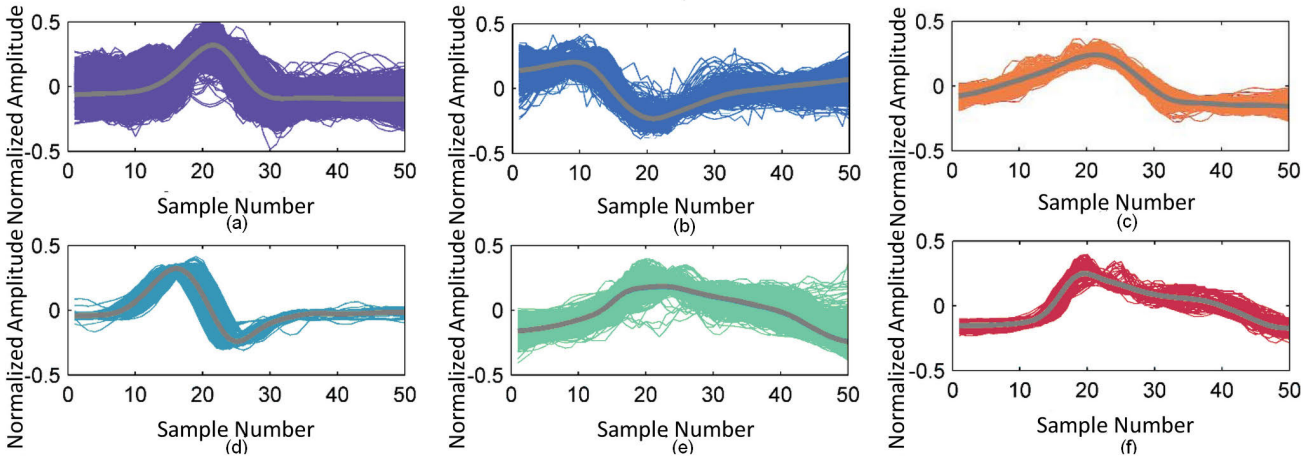

FIGURE 11. Examples of extracted visual morphological patterns of QRS complex for heartbeats from the MITDB. Gray line represents the centroid of each pattern; while lines in other colors represent original QRS complex segments assigned to the corresponding patterns.

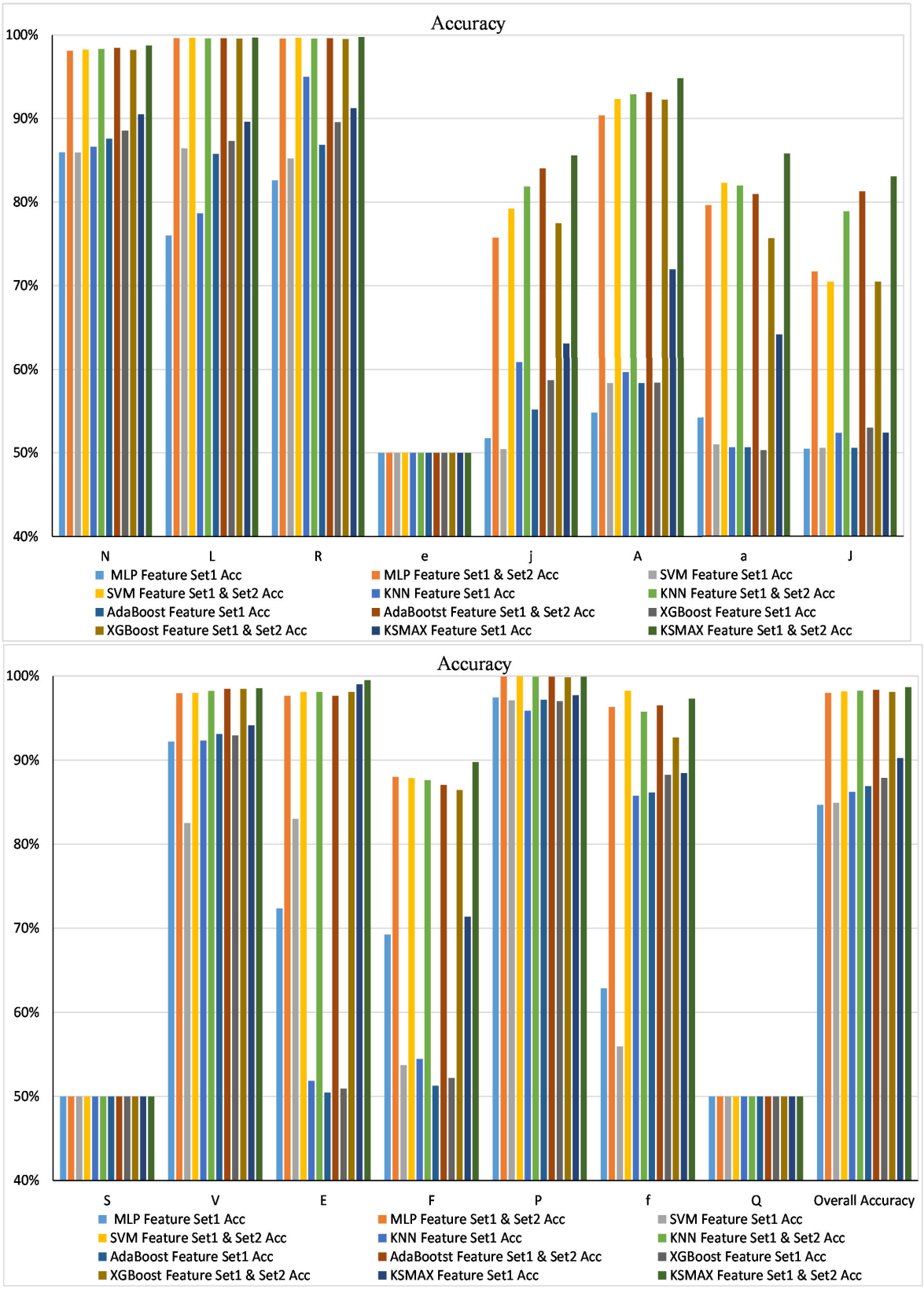

FIGURE 12. Comparison of accuracy achieved using combinations of feature sets and different classifiers (KNN, SVM, MLP, AdaBoost, XGBoost, and KSMAX) in terms of heartbeat type and accuracy.

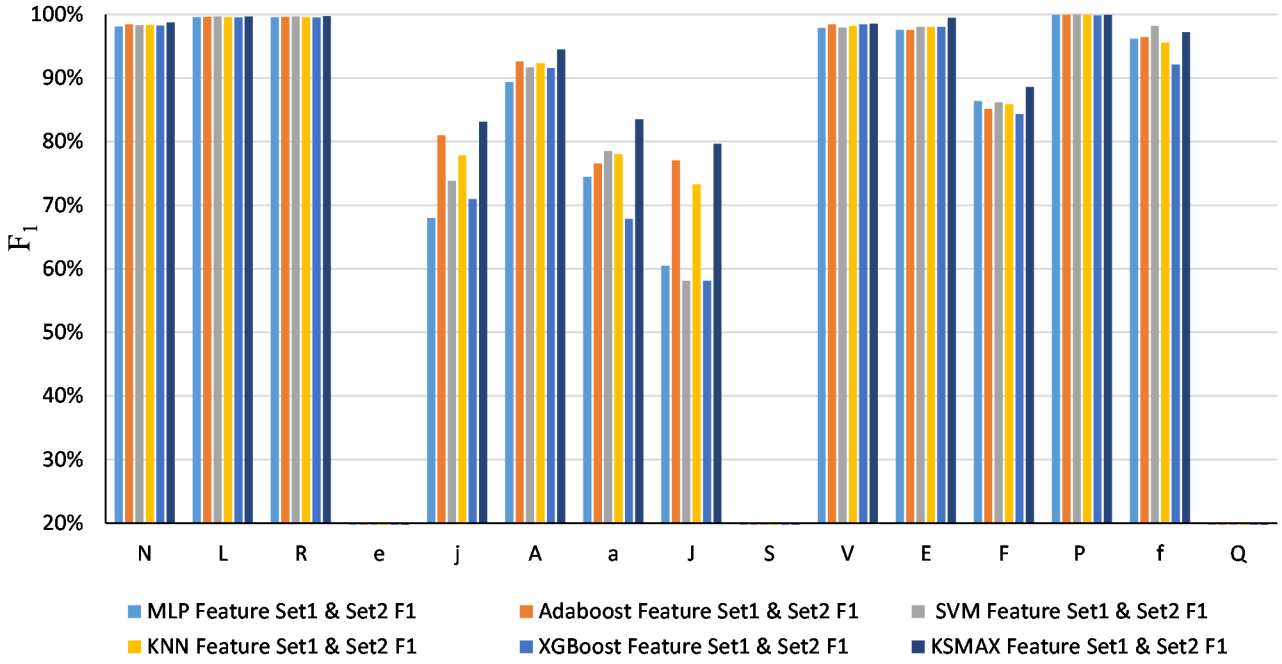

FIGURE 13. Comparison of F_1 achieved using the proposed feature set and different classifiers (KNN, SVM, MLP, AdaBoost, XGBoost, and KSMAX) in terms of heartbeat type.

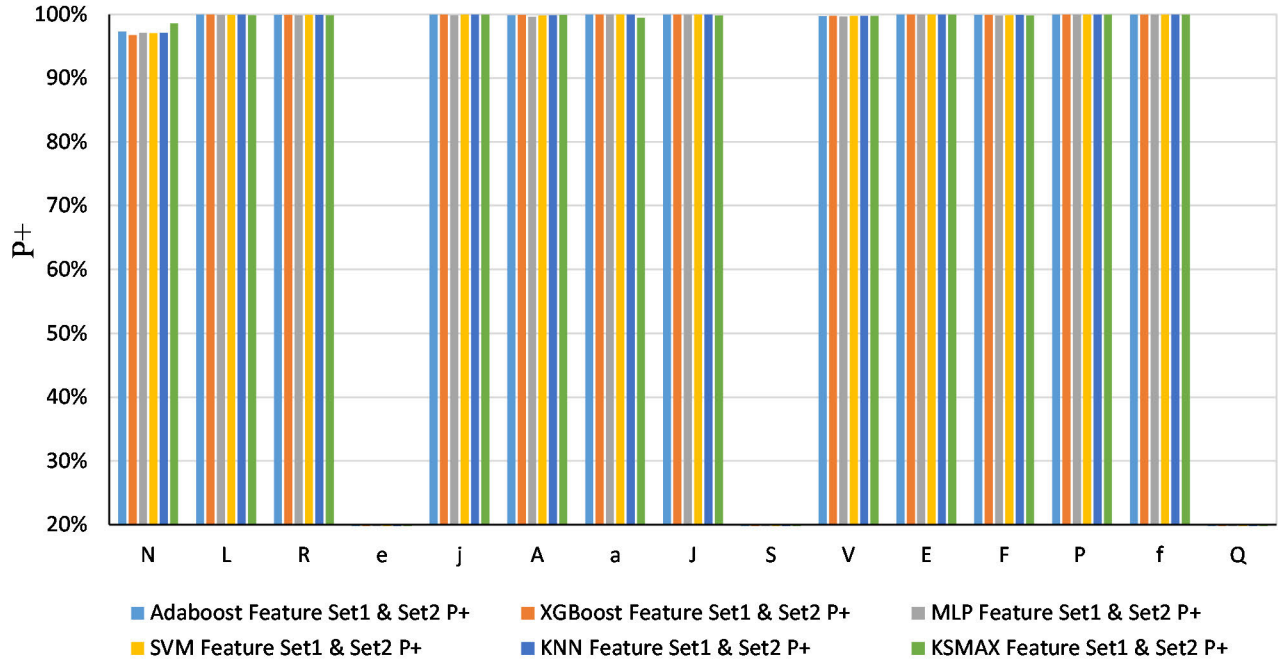

FIGURE 14. Comparison of P+ achieved using the proposed feature set and different classifiers (KNN, SVM, MLP, AdaBoost, XGBoost, and KSMAX) in terms of heartbeat type.

XGBoost, a remarkable increase of 15.69% in F_1 score was achieved using the proposed KSMAX classifier for aberrated atrial premature (a) type. As to the P+ measures, there was a notably improvement for normal (N) type which accounts for 71.17% of all the instances. Although the performance of the KSMAX in P+ measure for the rest heartbeat types was very close to the component classifiers in Fig. 14, when it comes to the F_1 score which takes both Recall and P+ into account, the result implies that our proposed approach is superior to MLP, SVM, KNN, AdaBoost, and XGBoost. Moreover, a better generalization capability is achieved through an ensemble of these diverse and strong component classifiers. Consequently, the reliability and accuracy of the proposed approach is further justified.

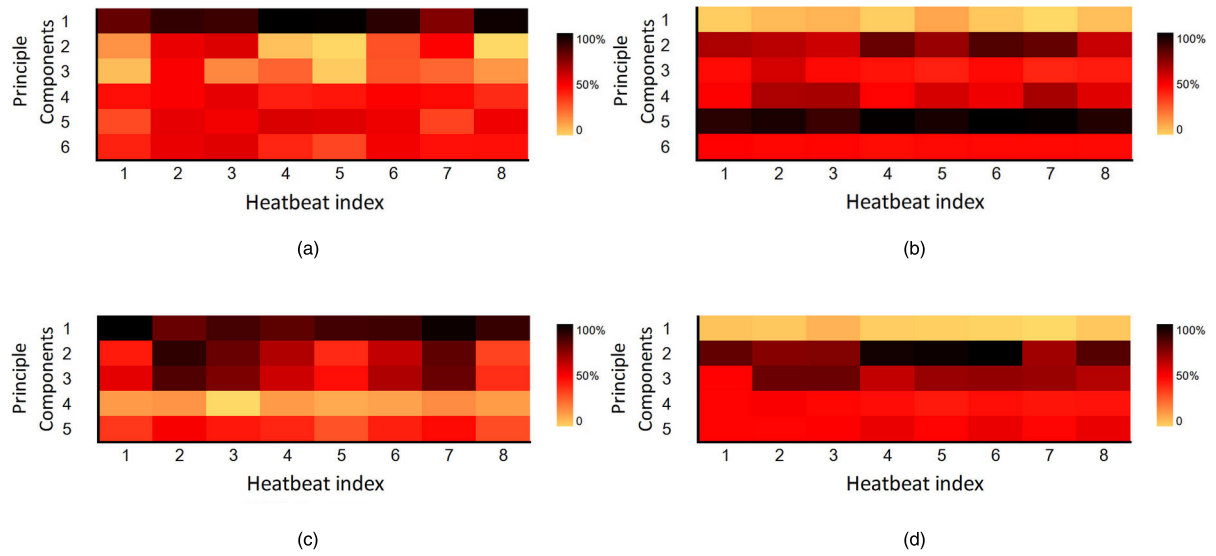

FIGURE 15. Heatmaps of the extracted principle components from third-level detail coefficients of eight normal heartbeats (a) and eight premature ventricular contraction heartbeats (b); and those from fourth-level detail coefficients of eight normal heartbeats (c), and eight premature ventricular contraction heartbeats (d), respectively.

TABLE 3. A summary of the accuracy achieved using component classifiers and the proposed KSMAX based on feature set1 (FS 1) and our proposed feature set1 & set2 (FS 1&2), respectively.

Types	MLP		SVM		KNN		AdaBoost		XGBoost		KSMAX	
	FS 1 Acc(%)	FS 1&2 Acc(%)	FS 1 Acc(%)	FS 1&2 Acc(%)	FS 1 Acc(%)	FS 1&2 Acc(%)	FS 1 Acc(%)	FS 1&2 Acc(%)	FS 1 Acc(%)	FS 1&2 Acc(%)	FS 1 Acc(%)	FS 1&2 Acc(%)
N	85.97	98.11	85.94	98.27	86.64	98.35	87.58	98.46	88.56	98.22	90.50	98.75
L	75.99	99.62	86.43	99.68	78.68	99.60	85.78	99.63	87.32	99.57	89.61	99.70
R	82.62	99.59	85.23	99.68	95.03	99.59	86.85	99.63	89.56	99.53	91.23	99.77
e	50.00	50.00	50.00	50.00	50.00	50.00	50.00	50.00	50.00	50.00	50.00	50.00
j	51.74	75.73	50.44	79.25	60.89	81.87	55.23	84.05	58.71	77.51	63.09	85.58
A	54.84	90.37	58.36	92.31	59.68	92.89	58.36	93.12	58.41	92.24	71.95	94.81
a	54.27	79.66	51.00	82.33	50.66	82.00	50.67	81.00	50.33	75.67	64.17	85.81
J	50.50	71.68	50.60	70.48	52.40	78.91	50.60	81.32	53.01	70.48	52.41	83.08
S	50.00	50.00	50.00	50.00	50.00	50.00	50.00	50.00	50.00	50.00	50.00	50.00
V	92.20	97.98	82.53	97.99	92.34	98.25	93.13	98.48	92.94	98.48	94.16	98.57
E	72.39	97.64	83.02	98.11	51.88	98.11	50.47	97.64	50.94	98.11	99.04	99.52
F	69.28	88.03	53.74	87.87	54.46	87.62	51.29	87.07	52.22	86.45	71.37	89.78
P	97.46	99.95	97.12	99.97	95.89	99.93	97.19	99.93	97.02	99.86	97.73	99.94
f	62.87	96.34	55.96	98.26	85.76	95.77	86.15	96.54	88.27	92.69	88.46	97.31
Q	50.00	50.00	50.00	50.00	50.00	50.00	50.00	50.00	50.00	50.00	50.00	50.00
Overall Accuracy	84.68	98.00	84.93	98.19	86.23	98.27	86.91	98.37	87.91	98.13	90.25	**98.68**

However, since there are very limited instances of atrial escape type (e), supraventricular premature type (S), and unclassifiable type (Q) in the MITDB, it is insufficient for completing a reliable learning. Thus, all the classifiers involved reported limited results with these types.

B. A COMPARISON WITH RECENT APPROACHES

The comparison of this work with relevant peerworks, in terms of the feature, classifier, data size, type number, and accuracy, is reported in Table 5.

In [28] and [48], ensemble algorithm obtained a higher accuracy (95%) than neural system when they were both

TABLE 4. A summary of statistical indicators using the proposed feature set and KSMAX classifier in the assessment. The metrics are: F_1 score (F_1) and precision (P+).

KSMAX	(%)	N	L	R	e	j	A	a	J	S	V	E	F	P	f	Q
Proposed	F_1	98.75	99.70	99.77	-	83.16	94.53	83.53	79.66	-	98.55	99.52	88.63	99.94	97.23	-
	P+	98.59	99.86	99.86	0	99.98	99.91	99.47	99.83	-	99.78	99.99	99.85	99.99	100	0

TABLE 5. Comparison of the classification performance of the proposed method with recent approaches.

Authors	Year	Feature	Classifier	Type	Data Size	Accuracy
Pławiak *et al*. [28]	2018	Frequency Components of the PSD	Evolutionary Neural System (based on single SVM)	15	1000 (segments)	91.00%
Venkatesan *et al*. [63]	2018	HRV Parameters	SVM	2	N/A	96.00%
Oh *et al*. [50]	2018	Normalized ECG Data	CNN+LSTM	5	16499 (segments)	98.10%
Marinho *et al*. [16]	2019	SCM+Fourier+HOS+Goertzel	Bayes	5	100467	94.30%
Yang *et al*. [45]	2019	Raw Data	DL-CCANeT	15	3350	95.25%
Pławiak *et al*. [48]	2019	Frequency Components of the PSD	Deep Genetic Ensemble of Classifiers	17	744 (segments)	95.00%
Liu *et al*. [64]	2020	Bispectrum+2D-Graph Fourier Transform	SVM-RBF	4	75604	96.20%
This study	2021	Parameter +VMP-QRS +PCA+DWT	KSMAX	15	104986	98.68%

trained with power spectral density (PSD). Literature [63] applied SVM in discriminating abnormal heartbeats from normal heartbeats and obtained a highest accuracy of 96.00%. Literature [50] reported a method combing CNN and LSTM techniques could categorize five types of heartbeats with 98.10% accuracy. In [45], DL-CCANet was proposed to classify 3350 heartbeats and obtained a 95.20% overall accuracy. The method proposed by Liu *et al*. [64] achieved an accuracy of 96.25% for classifying four classes of beats using SVM-RBF along with bispectrum and 2D-graph Fourier transform features.

In order to make a fair comparison, two items should be noted. First, the data size influences the evaluation result of the method. Second, the number of heartbeat types matters. In our work, the validity of the proposed approach was evaluated with 104986 heartbeats from MITDB. In addition, the assessment adopted all the heartbeat types listed in AAMI standard. Since the proposed approach has been evaluated with the widely-used evaluation measure (i.e., Acc) in literature considering the aspects discussed above, the results can be more similar to what it would produce when applied in real clinical practice. Therefore, from comparison of this work with peer works, it can be verified that the proposed approach outperforms the other methods.

Besides as wearable IoT devices that include ECG acquisition (e.g. smart watches and smart t-shirt) are becoming more and more popular, the proposed approach would be feasible and reliable when serving as a ubiquitous medical system for diagnosis of heart ventricular and atrial abnormalities due to the advantages of no stress of prohibitively expensive hardware, reduced set of features, and fewer parameters to set up.

V. CONCLUSION

In this paper, we propose an effective approach for detection of heart ventricular and atrial abnormalities. Each heartbeat is represented by a feature vector consisting of morphological parameters, principle components of the third-level and fourth-level detail coefficients of a four-level DWT decomposition, as well as VMP-QRS. In addition,

a novel classification algorithm, KSMAX, is proposed through an ensemble of five algorithms: KNN, SVM, MLP, AdaBoost, and XGBoost, which are heterogeneous and diverse in structures and theories. The proposed approach was validated on fifteen heartbeat types from MITDB, according to AAMI standard and obtained 98.68% overall accuracy. The accuracies for the six main types, namely, N, L, R, V, A, and P were 98.75%, 99.70%, 99.77%, 98.57%, 94.81%, and 99.94%, respectively. The proposed approach is then compared with some peer works and proves a higher accuracy in heart atrial and ventricular abnormalities detection scenario.

Due to the solid result achieved, the methodology in this study can be used in the research and development of cardiac arrhythmia detection system and telemedicine applications. Since the extracted features are mostly associated with physiological meaning, it is easy for physicians to comprehend intuitively and would effectively reduce the workload of manual examination of the long-term ECG recordings.

Since we mainly utilized some of the algorithms which have been frequently reported to yield promising results for this task, as our component classifiers, many other classifiers are out of scope. In addition, the principle components and visual patterns were extracted from the most significant wave in ECG signal. Further study should investigate the performance improvement by involving more ECG segments and other classification algorithms. In addition, more ECG records for rare heartbeat types should be collected in future to further improve the performance of the proposed system. Finally, the application of Local Interpretable Model-Agnostic Explanations (LIME) framework [66], [67] which might help adding some form of interpretability in the classification algorithm would be recommended as future work.

REFERENCES

[1] World Health Organization. (2018). *World Health Statistics 2018: Monitoring health for the SDGs, Sustainable Development Goals*. Geneva, Switzerland. Accessed: Jun. 5, 2020. [Online]. Available: https://www.who.int/health-topics/cardiovascular-diseases/

[2] B. Hemmeryckx, Y. Feng, L. Frederix, M. Lox, S. Trenson, R. Vreeken, H. R. Lu, D. Gallacher, Y. Ni, and H. R. Lijnen, "Evaluation of cardiac arrhythmic risks using a rabbit model of left ventricular systolic dysfunction," *Eur. J. Pharmacol.*, vol. 832, pp. 145–155, Aug. 2018.

[3] S. H. Jambukia, V. K. Dabhi, and H. B. Prajapati, "Classification of ECG signals using machine learning techniques: A survey," in *Proc. Int. Conf. Adv. Comput. Eng. Appl.*, Mar. 2015, pp. 714–721.

[4] P. E. McSharry, G. D. Clifford, L. Tarassenko, and L. A. Smith, "A dynamical model for generating synthetic electrocardiogram signals," *IEEE Trans. Biomed. Eng.*, vol. 50, no. 3, pp. 289–294, Mar. 2003.

[5] L. Wang, W. Sun, Y. Chen, P. Li, and L. Zhao, "Wavelet transform based ECG denoising using adaptive thresholding," in *Proc. 7th Int. Conf. Bioinf. Biomed. Sci. (ICBBS)*, Jun. 2018, pp. 35–40.

[6] W.-H. Jung and S.-G. Lee, "ECG identification based on non-fiducial feature extraction using window removal method," *Appl. Sci.*, vol. 7, no. 11, p. 1205, Nov. 2017, doi: 10.3390/app7111205.

[7] A. M. Alqudah, A. Albadarneh, I. Abu-Qasmieh, and H. Alquran, "Developing of robust and high accurate ECG beat classification by combining Gaussian mixtures and wavelets features," *Australas. Phys. Eng. Sci. Med.*, vol. 42, no. 1, pp. 149–157, Mar. 2019.

[8] M. Rakshit and S. Das, "An efficient ECG denoising methodology using empirical mode decomposition and adaptive switching mean filter," *Biomed. Signal Process. Control*, vol. 40, pp. 140–148, Feb. 2018.

[9] S. Poungponsri and X.-H. Yu, "An adaptive filtering approach for electrocardiogram (ECG) signal noise reduction using neural networks," *Neurocomputing*, vol. 117, pp. 206–213, Oct. 2013.

[10] T. He, G. Clifford, and L. Tarassenko, "Application of independent component analysis in removing artefacts from the electrocardiogram," *Neural Comput. Appl.*, vol. 15, no. 2, pp. 105–116, Apr. 2006.

[11] C.-C. Lin and C.-M. Yang, "Heartbeat classification using normalized RR intervals and morphological features," *Math. Problems Eng.*, vol. 2014, pp. 1–11, May 2014.

[12] P. deChazal, M. O'Dwyer, and R. B. Reilly, "Automatic classification of heartbeats using ECG morphology and heartbeat interval features," *IEEE Trans. Biomed. Eng.*, vol. 51, no. 7, pp. 1196–1206, Jul. 2004.

[13] M. Llamedo and J. P. Martínez, "Heartbeat classification using feature selection driven by database generalization criteria," *IEEE Trans. Biomed. Eng.*, vol. 58, no. 3, pp. 616–625, Mar. 2011.

[14] M. G. Tsipouras and D. I. Fotiadis, "Automatic arrhythmia detection based on time and time–frequency analysis of heart rate variability," *Comput. Methods Programs Biomed.*, vol. 74, no. 2, pp. 95–108, May 2004.

[15] U. R. Acharya, P. S. Bhat, S. S. Iyengar, A. Rao, and S. Dua, "Classification of heart rate data using artificial neural network and fuzzy equivalence relation," *Pattern Recognit.*, vol. 36, no. 1, pp. 61–68, Jan. 2003.

[16] L. B. Marinho, N. D. M. M. Nascimento, J. W. M. Souza, M. V. Gurgel, P. P. R. Filho, and V. H. C. de Albuquerque, "A novel electrocardiogram feature extraction approach for cardiac arrhythmia classification," *Future Gener. Comput. Syst.*, vol. 97, pp. 564–577, Aug. 2019.

[17] Y. Özbay and G. Tezel, "A new method for classification of ECG arrhythmias using neural network with adaptive activation function," *Digit. Signal Process.*, vol. 20, no. 4, pp. 1040–1049, Jul. 2010.

[18] E. Naseri, A. Ghaffari, and M. Abdollahzade, "A novel ICA-based clustering algorithm for heart arrhythmia diagnosis," *Pattern Anal. Appl.*, vol. 22, no. 2, pp. 285–297, May 2019.

[19] M. Korürek and B. Doğan, "ECG beat classification using particle swarm optimization and radial basis function neural network," *Expert Syst. Appl.*, vol. 37, no. 12, pp. 7563–7569, Dec. 2010.

[20] R. G. Afkhami, G. Azarnia, and M. A. Tinati, "Cardiac arrhythmia classification using statistical and mixture modeling features of ECG signals," *Pattern Recognit. Lett.*, vol. 70, pp. 45–51, Jan. 2016.

[21] Z. Zhang, J. Dong, X. Luo, K.-S. Choi, and X. Wu, "Heartbeat classification using disease-specific feature selection," *Comput. Biol. Med.*, vol. 46, pp. 79–89, Mar. 2014.

[22] C.-H. Lin, "Frequency-domain features for ECG beat discrimination using grey relational analysis-based classifier," *Comput. Math. Appl.*, vol. 55, no. 4, pp. 680–690, Feb. 2008.

[23] C. Lin, Y. Du, and T. Chen, "Adaptive wavelet network for multiple cardiac arrhythmias recognition," *Expert Syst. Appl.*, vol. 34, no. 4, pp. 2601–2611, May 2008.

[24] Y. Kutlu and D. Kuntalp, "Feature extraction for ECG heartbeats using higher order statistics of WPD coefficients," *Comput. Methods Programs Biomed.*, vol. 105, no. 3, pp. 257–267, Mar. 2012.

[25] T. Tuncer, S. Dogan, P. Pławiak, and U. R. Acharya, "Automated arrhythmia detection using novel hexadecimal local pattern and multilevel wavelet transform with ECG signals," *Knowl.-Based Syst.*, vol. 186, Dec. 2019, Art. no. 104923, doi: 10.1016/j.knosys.2019.104923.

[26] A. Daamouche, L. Hamami, N. Alajlan, and F. Melgani, "A wavelet optimization approach for ECG signal classification," *Biomed. Signal Process. Control*, vol. 7, no. 4, pp. 342–349, Jul. 2012.

[27] S. Kara and M. Okandan, "Atrial fibrillation classification with artificial neural networks," *Pattern Recognit.*, vol. 40, no. 11, pp. 2967–2973, Nov. 2007.

[28] P. Pławiak, "Novel methodology of cardiac health recognition based on ECG signals and evolutionary-neural system," *Expert Syst. Appl.*, vol. 92, pp. 334–349, Feb. 2018.

[29] R. J. Martis, U. R. Acharya, K. M. Mandana, A. K. Ray, and C. Chakraborty, "Cardiac decision making using higher order spectra," *Biomed. Signal Process. Control*, vol. 8, no. 2, pp. 193–203, Mar. 2013.

[30] S.-N. Yu and Y.-H. Chen, "Electrocardiogram beat classification based on wavelet transformation and probabilistic neural network," *Pattern Recognit. Lett.*, vol. 28, no. 10, pp. 1142–1150, Jul. 2007.

[31] Y. Kaya and H. Pehlivan, "Classification of premature ventricular contraction in ECG," *Int. J. Adv. Comput. Sci. Appl.*, vol. 6, no. 7, pp. 34–40, 2015.

[32] C. Ye, M. T. Coimbra, and B. V. K. V. Kumar, "Arrhythmia detection and classification using morphological and dynamic features of ECG signals," in *Proc. Annu. Int. Conf. IEEE Eng. Med. Biol.*, Aug. 2010, pp. 1918–1921.

[33] M. P. S. Chawla, "A comparative analysis of principal component and independent component techniques for electrocardiograms," *Neural Comput. Appl.*, vol. 18, no. 6, pp. 539–556, Sep. 2009.
[34] R. J. Martis, U. R. Acharya, and L. C. Min, "ECG beat classification using PCA, LDA, ICA and discrete wavelet transform," *Biomed. Signal Process. Control*, vol. 8, no. 5, pp. 437–448, Sep. 2013.
[35] C. Amuthadevi, "Effective ECG beat classification using colliding bodies," *Biomed. Res.*, vol. 28, pp. 307–314, Mar. 2017.
[36] R. J. Martis, U. R. Acharya, C. M. Lim, K. M. Mandana, A. K. Ray, and C. Chakraborty, "Application of higher order cumulant features for cardiac health diagnosis using ECG signals," *Int. J. Neural Syst.*, vol. 23, no. 4, Aug. 2013, Art. no. 1350014.
[37] A. F. Khalaf, M. I. Owis, and I. A. Yassine, "A novel technique for cardiac arrhythmia classification using spectral correlation and support vector machines," *Expert Syst. Appl.*, vol. 42, no. 21, pp. 8361–8368, Nov. 2015.
[38] M. Thomas, M. K. Das, and S. Ari, "Automatic ECG arrhythmia classification using dual tree complex wavelet based features," *AEU Int. J. Electron. Commun.*, vol. 69, no. 4, pp. 715–721, Apr. 2015.
[39] M. A. Escalona-Morán, M. C. Soriano, I. Fischer, and C. R. Mirasso, "Electrocardiogram classification using reservoir computing with logistic regression," *IEEE J. Biomed. Health Informat.*, vol. 19, no. 3, pp. 892–898, May 2015.
[40] I. Christov, V. Krasteva, I. Simova, T. Neycheva, and R. Schmid, "Multiparametric analysis for atrial fibrillation classification in the ECG," in *Proc. Comput. Cardiol. Conf. (CinC)*, Sep. 2017, pp. 1–4.
[41] N. Razmjooy, M. Ramezani, and N. Ghadimi, "Imperialist competitive algorithm-based optimization of neuro-fuzzy system parameters for automatic red-eye removal," *Int. J. Fuzzy Syst.*, vol. 19, no. 4, pp. 1144–1156, Mar. 2017, doi: 10.1007/s40815-017-0305-2.
[42] Y. Kaya, H. Pehlivan, and M. E. Tenekeci, "Effective ECG beat classification using higher order statistic features and genetic feature selection," *Biomed. Res.*, vol. 28, no. 17, pp. 7594–7603, 2017.
[43] C. K. Jha and M. H. Kolekar, "Cardiac arrhythmia classification using tunable Q-wavelet transform based features and support vector machine classifier," *Biomed. Signal Process. Control*, vol. 59, May 2020, Art. no. 101875.
[44] M. Mohanty, S. Sahoo, P. Biswal, and S. Sabut, "Efficient classification of ventricular arrhythmias using feature selection and C4.5 classifier," *Biomed. Signal Process. Control*, vol. 44, pp. 200–208, Jul. 2018.
[45] W. Yang, Y. Si, D. Wang, and G. Zhang, "A novel approach for multi-lead ECG classification using DL-CCANet and TL-CCANet," *Sensors*, vol. 19, no. 14, p. 3214, Jul. 2019.
[46] S. L. Oh, E. Y. K. Ng, R. S. Tan, and U. R. Acharya, "Automated diagnosis of arrhythmia using combination of CNN and LSTM techniques with variable length heart beats," *Comput. Biol. Med.*, vol. 102, pp. 278–287, Nov. 2018.
[47] L. Qian, J. Wang, L. Jin, Y. Huang, J. Zhang, H. Zhu, S. Yan, and X. Wu, "Optimized convolutional neural network by genetic algorithm for the classification of complex arrhythmia," *J. Med. Imag. Health Inform.*, vol. 9, no. 9, pp. 1905–1912, Dec. 2019.
[48] P. Pławiak and U. R. Acharya, "Novel deep genetic ensemble of classifiers for arrhythmia detection using ECG signals," *Neural Comput. Appl., pp. 1–25, Jan.*, vol. 2019, doi: 10.1007/s00521-018-03980-2.
[49] S. M. Mathews, C. Kambhamettu, and K. E. Barner, "A novel application of deep learning for single-lead ECG classification," *Comput. Biol. Med.*, vol. 99, pp. 53–62, Aug. 2018.
[50] J. Pan and W. J. Tompkins, "A real-time QRS detection algorithm," *IEEE Trans. Biomed. Eng.*, vol. BME-32, no. 3, pp. 230–236, Mar. 1985.
[51] H. Yang and Z. Wei, "Arrhythmia recognition and classification using combined parametric and visual pattern features of ECG morphology," *IEEE Access*, vol. 8, pp. 47103–47117, 2020.
[52] E. J. D. S. Luz, W. R. Schwartz, G. Cámara-Chávez, and D. Menotti, "ECG-based heartbeat classification for arrhythmia detection: A survey," *Comput. Methods Programs Biomed.*, vol. 127, pp. 144–164, Apr. 2016.
[53] A. L. Goldberger, L. A. N. Amaral, L. Glass, J. M. Hausdorff, P. C. Ivanov, R. G. Mark, J. E. Mietus, G. B. Moody, C.-K. Peng, and H. E. Stanley, "PhysioBank, PhysioToolkit, and PhysioNet: Components of a new research resource for complex physiologic signals," *Circulation*, vol. 101, no. 23, Jun. 2000.
[54] J. Schmidhuber, "Deep learning in neural networks: An overview," *Neural Netw.*, vol. 61, pp. 85–117, Jan. 2015.
[55] C. M. Bishop, *Pattern Recognition and Machine Learning*. Berlin, Germany: Springer, 2007, pp. 236–240.
[56] J. Kivinen, A. J. Smola, and R. C. Williamson, "Learning with Kernels," *IEEE Trans. Signal Process.*, vol. 52, no. 8, pp. 2165–2176, Jul. 2004.
[57] C.-C. Chang and C.-J. Lin, "LIBSVM: A library for support vector machines," *ACM Trans. Intell. Syst. Technol.*, vol. 2, no. 3, pp. 1–27, Apr. 2011.
[58] M.-A. Amal and B.-A. Ahmed, "Survey of nearest neighbor condensing techniques," *Int. J. Adv. Comput. Sci. Appl.*, vol. 2, no. 11, pp. 302–305, 2011.
[59] Y. Freund and R. E. Schapire, "A decision-theoretic generalization of on-line learning and an application to boosting," in *Proc. 2nd Eur. Conf. Comput. Learn. Theory (EuroCOLT)*, Berlin, Germany, Jun. 1995, pp. 23–37, doi: 10.1007/3-540-59119-2_166.
[60] T. Chen and C. Guestrin, "XGBoost: A scalable tree boosting system," in *Proc. 22nd ACM SIGKDD Int. Conf. Knowl. Discovery Data Mining*, Aug. 2016, pp. 785–794.
[61] J. Large, J. Lines, and A. Bagnall, "A probabilistic classifier ensemble weighting scheme based on cross-validated accuracy estimates," *Data Mining Knowl. Discovery*, vol. 33, no. 6, pp. 1674–1709, Jun. 2019.
[62] *ANSI/AAMI, Testing and Reporting Performance Results of Cardiac Rhythm and ST Segment Measurement Algorithms*, document ANSI/AAMI/ISO EC57, 1998-(R)2008, American National Standards Institute, Inc. (ANSI), Association for the Advancement of Medical Instrumentation (AAMI), 2008.
[63] C. Venkatesan, P. Karthigaikumar, A. Paul, S. Satheeskumaran, and R. Kumar, "ECG signal preprocessing and SVM classifier-based abnormality detection in remote healthcare applications," *IEEE Access*, vol. 6, pp. 9767–9773, 2018.
[64] S. Liu, J. Shao, T. Kong, and R. Malekian, "ECG arrhythmia classification using high order spectrum and 2D graph Fourier transform," *Appl. Sci.*, vol. 10, no. 14, p. 4741, Jul. 2020.
[65] G. Sannino and G. De Pietro, "A deep learning approach for ecg-based heartbeatclassification for arrhythmia detection," *Future Gener. Comput. Syst.*, vol. 86, pp. 446–455, Sep. 2018.
[66] J.-M. Fellous, G. Sapiro, A. Rossi, H. Mayberg, and M. Ferrante, "Explainable artificial intelligence for neuroscience: Behavioral neurostimulation," *Frontiers Neurosci.*, vol. 13, p. 1346, Dec. 2019.
[67] S. M. Mathews, "Explainable artificial intelligence applications in NLP, biomedical, and malware classification: A literature review," in *Proc. Intell. Comput. (CompCom)*, London, U.K., Jul. 2019, pp. 1269–1292.

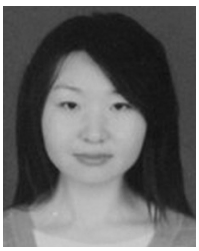

HUI YANG (Member, IEEE) received the B.Eng. degree in applied electronics technology from Qingdao Ocean University (currently Ocean University of China), Qingdao, China, in 2002, the M.Sc. degree in advanced photonics and communications from the University of Warwick, Coventry, U.K., in 2005, and the Ph.D. degree in computer software and theory from the Ocean University of China, in 2021. Since 2006, she has been working with the Department of Computer Foundation, Ocean University of China, where she is currently a Lecturer. Her research interests include signal processing, machine learning, and intelligent computing.

ZHIQIANG WEI received the B.Eng. degree from Shandong University, Jinan, China, in 1992, the M.Sc. degree from the Harbin Institute of Technology, Harbin, China, in 1995, and the Ph.D. degree from Tsinghua University, Beijing, China, in 2001. He is currently a Professor with the Ocean University of China. His main research interests include signal processing, software engineering, and intelligent computing.